

CLRCNTR: A Color Contour Plotting Routine for Displaying CFD-Generated Solutions



Robert L. Spinetti
Calspan Corporation

April 1987

Final Report for Period October 1, 1985 – September 30, 1986

Approved for public release; distribution is unlimited.

**TECHNICAL REPORTS
FILE COPY**

**ARNOLD ENGINEERING DEVELOPMENT CENTER
ARNOLD AIR FORCE STATION, TENNESSEE
AIR FORCE SYSTEMS COMMAND
UNITED STATES AIR FORCE**

PROPERTY OF U.S. AIR FORCE
AEDC TECHNICAL LIBRARY

NOTICES

When U. S. Government drawings, specifications, or other data are used for any purpose other than a definitely related Government procurement operation, the Government thereby incurs no responsibility nor any obligation whatsoever, and the fact that the Government may have formulated, furnished, or in any way supplied the said drawings, specifications, or other data, is not to be regarded by implication or otherwise, or in any manner licensing the holder or any other person or corporation, or conveying any rights or permission to manufacture, use, or sell any patented invention that may in any way be related thereto.

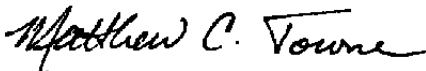
Qualified users may obtain copies of this report from the Defense Technical Information Center.

References to named commercial products in this report are not to be considered in any sense as an endorsement of the product by the United States Air Force or the Government.

This report has been reviewed by the Office of Public Affairs (PA) and is releasable to the National Technical Information Service (NTIS). At NTIS, it will be available to the general public, including foreign nations.

APPROVAL STATEMENT

This report has been reviewed and approved.



MATTHEW C. TOWNE, Capt, USAF
Facility Technology Division
Directorate of Technology
Deputy for Operations

Approved for publication:

FOR THE COMMANDER



MARION L. LASTER
Director of Technology
Deputy for Operations

UNCLASSIFIED

SECURITY CLASSIFICATION OF THIS PAGE

REPORT DOCUMENTATION PAGE

1a. REPORT SECURITY CLASSIFICATION UNCLASSIFIED			1b. RESTRICTIVE MARKINGS		
2a. SECURITY CLASSIFICATION AUTHORITY			3. DISTRIBUTION/AVAILABILITY OF REPORT Approved for public release; distribution is unlimited.		
2b. DECLASSIFICATION/DOWNGRADING SCHEDULE					
4. PERFORMING ORGANIZATION REPORT NUMBER(S) AEDC-TR-86-40			5. MONITORING ORGANIZATION REPORT NUMBER(S)		
6a. NAME OF PERFORMING ORGANIZATION Arnold Engineering Development Center		6b. OFFICE SYMBOL (If applicable) DOT		7a. NAME OF MONITORING ORGANIZATION	
6c. ADDRESS (City, State and ZIP Code) Air Force Systems Command Arnold Air Force Station, TN 37389-5000				7b. ADDRESS (City, State and ZIP Code)	
8a. NAME OF FUNDING/SPONSORING ORGANIZATION Arnold Engineering Development Center		8b. OFFICE SYMBOL (If applicable) DO		9. PROCUREMENT INSTRUMENT IDENTIFICATION NUMBER	
8c. ADDRESS (City, State and ZIP Code) Air Force Systems Command Arnold Air Force Station, TN 37389-5000				10. SOURCE OF FUNDING NOS.	
11. TITLE (Include Security Classification) SEE REVERSE OF THIS PAGE				65807F	
12. PERSONAL AUTHOR(S) Spinetti, Robert L., Calspan Corporation, AEDC Division					
13a. TYPE OF REPORT Final		13b. TIME COVERED FROM 10/1/85 TO 9/30/86		14. DATE OF REPORT (Yr., Mo., Day) April 1987	
15. PAGE COUNT 60					
16. SUPPLEMENTARY NOTATION Available in Defense Technical Information Center (DTIC).					
17. COSATI CODES			18. SUBJECT TERMS (Continue on reverse if necessary and identify by block number)		
FIELD	GROUP	SUB. GR.	computational fluid dynamics color contours		
09	02		computer programs fluid dynamics		
20	04		(cont)		
19. ABSTRACT (Continue on reverse if necessary and identify by block number) A computer program for displaying flow-field color contour plots, generated from computational fluid dynamics (CFD) solutions, has been developed by extending the contour plotting option of the GENPLOT routine of Dr. R. G. Hindman. An algorithm for generating color-filled contour regions was developed for this extension and is described. The algorithm performs a detailed examination of the behavior of the dependent variable within the plotting domain to generate the contour regions and determines the relationship between these regions and their associated contour levels to assign the appropriate fill color to a particular region. Flow-field color contour plots generated from a hypersonic viscous shock-layer computation, a supersonic viscous blunt-fin computation, and a hypersonic viscous gas jet nosetip computation are presented to illustrate the capabilities and flexibility of the routine and to demonstrate that they can be used to aid the interpretation of CFD results.					
20. DISTRIBUTION/AVAILABILITY OF ABSTRACT UNCLASSIFIED/UNLIMITED <input type="checkbox"/> SAME AS RPT. <input checked="" type="checkbox"/> DTIC USERS <input type="checkbox"/>			21. ABSTRACT SECURITY CLASSIFICATION UNCLASSIFIED		
22a. NAME OF RESPONSIBLE INDIVIDUAL W. O. Cole			22b. TELEPHONE NUMBER (Include Area Code) (615) 454-7813		22c. OFFICE SYMBOL DOS

DD FORM 1473, 83 APR

EDITION OF 1 JAN 73 IS OBSOLETE.

UNCLASSIFIED

SECURITY CLASSIFICATION OF THIS PAGE

UNCLASSIFIED

SECURITY CLASSIFICATION OF THIS PAGE

11. TITLE

CLRCNTR: A Color Contour Plotting Routine for Displaying CFD-Generated Solutions

18. SUBJECT TERMS (Concluded)

flow visualization
color graphics
computer graphics
color plotting
contour plotting

UNCLASSIFIED

SECURITY CLASSIFICATION OF THIS PAGE

PREFACE

The work reported herein was performed by the Arnold Engineering Development Center (AEDC), Air Force Systems Command (AFSC). The Air Force Program Managers were Dr. K. L. Kushman and Captain M. C. Towne, DOT. This work was performed by the Calspan Corporation, AEDC Division, operating contractor for the aerospace flight dynamics testing efforts at the AEDC, AFSC, Arnold Air Force Station, Tennessee. The work was performed in the von Kármán Gas Dynamics Facility (VKF) under AEDC Project Number DB97VA (Calspan Project Number V32A-CD). This report documents the development and application of CLRCNTR, a computer program for displaying flow-field color contour plots generated from computational fluid dynamics (CFD) solutions. The research was performed from October 1, 1985 through September 30, 1986, and the manuscript was submitted for publication October 7, 1986.

CONTENTS

	<u>Page</u>
1.0 INTRODUCTION	5
1.1 Motivation	5
1.2 Background	6
2.0 PROGRAM DEVELOPMENT	6
2.1 Assumptions and Concepts	6
2.2 Generation of Contour Lines	9
2.3 Generation of Contour Regions	10
2.4 Contour Region Area Computation and Assignment of Colors	11
3.0 PROGRAM APPLICATIONS	13
3.1 Hypersonic Viscous Shock-Layer Flow Over a Hemisphere	13
3.2 Supersonic Viscous Flow Over a Blunt Fin Protruding From A Flat Plate	13
3.3 Hypersonic Viscous Gas Jet Nosetip Flow Field	13
4.0 DISCUSSION OF RESULTS	14
5.0 CONCLUDING REMARKS	15
REFERENCES	16

ILLUSTRATIONS

<u>Figure</u>	<u>Page</u>
1. Hypersonic Viscous Shock-Layer Flow Over a Hemisphere	19
2. Supersonic Viscous Flow Over a Blunt Fin Protruding from a Flat Plate (Fin Plane-of-Symmetry)	31
3. Supersonic Viscous Flow Over a Blunt Fin Protruding from a Flat Plate (Plate Surface)	39
4. Hypersonic Viscous Gas Jet Nosetip Flow	47
NOMENCLATURE	55

1.0 INTRODUCTION

1.1 MOTIVATION

It has long been recognized that flow visualization plays an important role in the understanding of complex fluid-flow behavior. Mach (Ref. 1) published, in 1887, the first photographs of a bow shock wave visualized by the schlieren technique, and he photographed a bullet in supersonic flight in 1893 with a device that is now known as the Mach-Zehnder interferometer. Reynolds (Ref. 2) used dyes during experiments in which he determined that the transition from laminar to turbulent flow occurs at a critical value of the Reynolds number (Re_{cr}). Prandtl and Tietjens (Ref. 3) used aluminum dust particles to visualize boundary-layer separation, and Wieselsberger (Ref. 4) used smoke to "see" the point of separation move downstream in the classical experiment of flow past a sphere to which a thin wire is attached to trip the boundary layer. Van Dyke (Ref. 5) has compiled numerous flow visualization photographs into a bound volume. They serve as excellent examples of the information that can be gleaned from visual experiments.

With the advent of the supercomputer, the fluid dynamicist now has the capability to use complex numerical techniques to solve approximations to the partial differential equations of fluid motion in a timely and efficient manner. At the AEDC, the approximations must be of such quality that when used in conjunction with experimental results accurate flow predictions for test planning, test data validation, and extrapolation of test facility results to flight conditions can be provided. In view of the fact that flow visualization is essential to the understanding and interpretation of experimental fluid dynamic results, it is also necessary to generate a picture of the computational results to comprehend the flow field created by the numerical simulation and to verify the correctness of the solution. Displaying the results from CFD codes using computer graphics generally is considered to be the most practical method to view and examine the solution of a computation. Deiwert and Rothmund (Ref. 6), for example, used computer graphics to examine the results of a three-dimensional (3-D) flow computation over a conical afterbody containing a jet. The oblique shock wave generated by the expanding jet plume, and the slip surface between the free stream and the jet were easily perceived. Chaussee, Rizk, and Buning (Ref. 7) analyzed a viscous flow computation over a space shuttle orbiter-like configuration using computer graphics, and Hung and Buning (Ref. 8) investigated the shock wave/boundary-layer interaction induced by a blunt fin protruding from a flat plate using CFD results in conjunction with computer graphics. Because of the complexity of these flow fields, the use of color helps to maintain the graphic clarity. Color helps the individual to differentiate objects and/or flow features. In addition, color facilitates interpretation by making flow gradients and embedded regions readily apparent. Buning and Steger (Ref. 9) give an excellent overview of the importance

of using computer graphics for displaying the results from CFD codes. They also discuss the need for advanced algorithms that automate the process of searching for significant flow attributes through huge CFD databases and the need for powerful computer graphics workstations that have the capability to rotate and translate three-dimensional graphic images in real time.

The objective of this report is to document the development and application of a computer program for displaying flow-field color contour plots generated from CFD solutions. The program has been interfaced with several CFD codes at AEDC, and typical results are presented.

1.2 BACKGROUND

An unpublished computer program was written by Dr. R. G. Hindman, currently with Iowa State University, to display graphically solutions generated by the modified Hung-MacCormack two-dimensional (2-D) Navier-Stokes compression ramp code (Ref. 10). The program, coined GENPLOT, is a highly flexible monochrome plotting routine that graphically reproduces the computational mesh, the computed velocity field in vector form, flow-field contour maps, and boundary data plots at the user's request. An effort was initiated at the AEDC in 1983 to develop a user-friendly color contour plotting program to be used routinely with CFD codes. This was accomplished by exploiting the work of Hindman and adopting state-of-the-art computer graphics hardware devices and software packages to enhance the features of the flow-field contour plotting option of GENPLOT. The resultant plotting routine, called CLRCNTR, uses the basic program architecture, contour generating logic, and input/output requirements of GENPLOT.

2.0 PROGRAM DEVELOPMENT

2.1 ASSUMPTIONS AND CONCEPTS

The basic assumptions made by CLRCNTR are that the input flow solution is generated by a perfect-gas computation and that the plotting domain is two-dimensional and is enclosed by four boundaries. These boundaries are considered to be part of the plotting domain and can be, for example, solid surfaces, planes of symmetry, inflow/outflow planes, or the outer edge of the computational domain. The input flow solution can be generated from either a 2-D or a 3-D simulation; however, if it is generated from a 3-D simulation, a 2-D slice through this flow field must be selected and defined as the plotting domain. The plotting domain must be configured in the following form:

J =	1	2	3	4	5	JMAX
K = KMAX	+	+	+	+	+	+	+	+	+	+	+	+	+	+	+	+	K = KMAX
.	+	+	+	+	+	+	+	+	+	+	+	+	+	+	+	+	.
.	+	+	+	+	+	+	+	+	+	+	+	+	+	+	+	+	.
.	+	+	+	+	+	+	+	+	+	+	+	+	+	+	+	+	.
.	+	+	+	+	+	+	+	+	+	+	+	+	+	+	+	+	.
.	+	+	+	+	+	+	+	+	+	+	+	+	+	+	+	+	.
.	+	+	+	+	+	+	+	+	+	+	+	+	+	+	+	+	.
.	+	+	+	+	+	+	+	+	+	+	+	+	+	+	+	+	.
.	+	+	+	+	+	+	+	+	+	+	+	+	+	+	+	+	.
.	+	+	+	+	+	+	+	+	+	+	+	+	+	+	+	+	.
.	+	+	+	+	+	+	+	+	+	+	+	+	+	+	+	+	.
K = 5	+	+	+	+	+	+	+	+	+	+	+	+	+	+	+	+	K = 5
K = 4	+	+	+	+	+	+	+	+	+	+	+	+	+	+	+	+	K = 4
K = 3	+	+	+	+	+	+	+	+	+	+	+	+	+	+	+	+	K = 3
K = 2	+	+	+	+	+	+	+	+	+	+	+	+	+	+	+	+	K = 2
K = 1	+	+	+	+	+	+	+	+	+	+	+	+	+	+	+	+	K = 1
J =	1	2	3	4	5	JMAX

where $J = 1$ to $JMAX$ are, for example, the number of grid points along a body surface over which the flow field is computed, and $K = 1$ to $KMAX$ are the number of grid points normal to this surface. The user must input the flow solution in a form that is consistent with this domain. The physical coordinates of each grid point and the solution vector at each grid point are then defined on this domain. The x and y coordinates of the grid points geometrically define the plane of the plotting domain, and the z coordinate is assumed to be normal to this surface. This coordinate system does not necessarily have to coincide with the coordinate system that is defined in the CFD code. The solution vector is of the form $\rho, \rho u, \rho v, \rho w, e_t$ where ρ is the local density; $\rho u, \rho v$, and ρw are the x, y , and z components of momentum, respectively; and e_t is the local total energy per unit volume of the flow. The solution vector defines the flow in its entirety, within the assumptions made in the CFD code, and other parameters may be computed from it. These parameters are specified by executing an interactive interrogation program prior to executing CLRCNTR. They must be selected from the following menu:

Parameter	Normalization Parameter
Static Pressure Coefficient	---
Static Pressure	$\rho_{\infty} U_{\infty}^2$
Density	ρ_{∞}
u-Velocity	U_{∞}
v-Velocity	U_{∞}
w-Velocity	U_{∞}
Static Temperature	$T_{0\infty}$
Entropy	$s_{\infty} \gamma M_{\infty}^2$
Total Enthalpy	$H_{0\infty}$
Total Pressure	$\rho_{\infty} U_{\infty}^2$
Total Velocity	U_{∞}
Magnitude of Vorticity	U_{∞}
Stream Function (2-D or Axisymmetric Flow Solution Only)	$\rho_{\infty} U_{\infty}$
Local Mach Number	----
User-Defined Parameter	----

The parameters are normalized as shown if the solution vector is nondimensionalized as follows:

$$\begin{aligned} & \rho/\rho_{\infty} \\ & \rho u/\rho_{\infty} U_{\infty} \\ & \rho v/\rho_{\infty} U_{\infty} \\ & \rho w/\rho_{\infty} U_{\infty} \\ & e/\rho_{\infty} U_{\infty}^2 \end{aligned}$$

The interrogation program also prompts the user for plot labels, label heights, and contour levels and requests if the user wants a legend displayed. A subset of the plotting domain also may be specified during execution of this program. In addition, one of four options may be selected to specify the contour levels; they are

1. plot "n" contour levels between the selected domain maximum and minimum values,
2. plot "n" contour levels between user-specified maximum and minimum values,
3. plot "n" user-specified contour levels, and
4. plot contour levels given by the equation

$$\text{min} + (I - 1) \times \text{delta} \quad (1)$$

for $I = 1, N$, where $N = (\text{max} - \text{min}) / \text{delta}$ and min, max, and delta are user inputs. The input supplied to the interrogation program is stored on an input file for subsequent use by CLRCNTR.

2.2 GENERATION OF CONTOUR LINES

Contour lines, by definition, must either start and end at any of the four boundaries that enclose the plotting domain or must start and end within the boundaries and close back on themselves. It is not a difficult task to determine the location of the contour lines if the value of the function that is to be plotted is known at each of the grid points in the domain and if the levels of the contour lines are specified. For each contour level, this procedure is as follows:

CLRCNTR begins at the grid point defined by the indices $(J = 1, K = 1)$ and examines the behavior of the function along the $K = 1$ boundary. When the value of the function at the grid point $(J, K = 1)$ is less than the current contour level, and the value of the function at the grid point $(J + 1, K = 1)$ is greater than the current contour level, a linear interpolation is performed to determine the approximate starting location of the contour line on this boundary. The procedure then moves into the grid cell defined by the corner points $(J, K = 1)$, $(J + 1, K = 1)$, $(J + 1, K = 2)$, and $(J, K = 2)$. An average value of the function is computed from the values at each of the corner points, and this average is presumed to be located at a point defined by the intersection of the two lines that bisect opposite sides of the cell. CLRCNTR then examines the behavior of the function between this averaged point and the corner points $(J, K = 1)$ and $(J + 1, K = 1)$. The contour line must cross either the line segment constructed between the averaged point and the point $(J, K = 1)$ or the line segment constructed between the averaged point and the point $(J + 1, K = 1)$. After the appropriate segment is established, a linear interpolation is performed again to determine the approximate crossing location of the contour line. CLRCNTR continues to monitor the behavior of the function within the current grid cell by examining the mathematical relationship between the averaged point and the corner points $(J, K = 2)$ and $(J + 1, K = 2)$. The relationship between adjacent corner points is examined also, and the contour line exits from the grid cell if it can; however, if it does not exit from the cell, additional line segments must be constructed between the averaged point and the corner points $(J, K = 2)$ and $(J + 1, K = 2)$. The appropriate crossing location is then determined by linear interpolation. This procedure continues until the contour line exits the current grid cell. After leaving the cell, the contour line either enters an adjacent grid cell, or ends on the originating boundary. If it enters an adjacent cell, the above procedure is repeated using the four corner points

that define this cell. CLRCNTR moves from grid cell to grid cell "tracing" the contour line through the plotting domain until a boundary is reached. The program then returns to the starting boundary of the contour line where it continues to "look" for additional contour lines having levels that are equivalent to the current contour level. After the $K = 1$ boundary is exhausted, CLRCNTR moves to the $J = JMAX$ boundary, and the procedure is repeated. After all four boundaries are examined for the start of contour lines that have levels equivalent to the current contour level, CLRCNTR moves to the interior (i.e. off the boundaries) of the plotting domain and searches for contour lines that close back on themselves. The internal grid cell procedure described earlier is used, employing local cell corner points. All contour lines within the resolution of the plotting domain and having a functional value equivalent to the current contour level are generated at the completion of this procedure. The entire procedure is repeated for subsequent contour levels until all levels are depleted.

2.3 GENERATION OF CONTOUR REGIONS

A contour region is defined as that region that is enclosed by one or more plotting domain boundaries and one or more contour lines that have the same contour level. (The one exception to this definition is a contour line that closes back on itself; a contour line of this type implicitly defines a contour region.) Each contour region is determined by specifying the points along the boundary of this region. For each contour level, these points are determined by using the following procedure:

CLRCNTR begins at the grid point defined by the indices ($J = 1, K = 1$) and searches along the $K = 1$ boundary for the first point of a contour line that has a value equivalent to the current contour level. The searching will continue on the $J = JMAX$ boundary if the first point is not found on the $K = 1$ boundary. When this point is located, the next grid point on the local plotting domain boundary becomes the first point on the boundary of the contour region. For example, if the first point of the contour line is between the grid points ($J, K = 1$) and ($J + 1, K = 1$), the first point on the boundary of the contour region is the grid point ($J + 1, K = 1$). CLRCNTR now begins to search for the last point of this contour line starting from the current location, for example, the point ($J + 1, K = 1$). The searching will continue on the $J = JMAX$ boundary if the last point is not found on the $K = 1$ boundary. All plotting domain boundary points become contour region boundary points until either the last point of the contour line is located or until the first point of a second contour line that has a value equivalent to the current contour level is found. If the first point of a second contour line is found before the last point

of the first contour line is located, the points that define the second contour line become points on the boundary of the contour region that is being generated. The second contour line terminates at one of the four plotting domain boundaries. CLRCNTR continues to search for the last point of the first contour line starting from this location. All plotting domain boundary points continue to become contour region boundary points. If subsequent contour lines that have a value equivalent to the current contour level are encountered before the last point of the first contour line is located, the points that define these lines also become points on the boundary of the current contour region. These subsequent contour lines terminate at a plotting domain boundary. CLRCNTR continues to search for the last point of the first contour line starting from this location. The region is completed after this point is found. The points that define the first contour line become contour region boundary points, and the region is closed with the first point of the first contour line. After this region is completed, CLRCNTR searches for any remaining contour lines at the current contour level and generates additional contour regions as required. The entire procedure is repeated for subsequent contour levels until all levels are depleted.

2.4 CONTOUR REGION AREA COMPUTATION AND ASSIGNMENT OF COLORS

The contour regions must be displayed in a specific sequence to construct the entire flow-field contour plot correctly. A simple example illustrating the problem that can be encountered if the regions are displayed in a random sequence is the embedding of one contour region within another. If a smaller region is embedded within a larger one, and the smaller region is displayed first, it will be erased when the larger region is displayed on top of it. This problem is resolved by displaying the region that has the larger area before displaying the region that has the smaller area. The areas are computed by applying Green's theorem to each contour region and evaluating the resulting line integral around its boundary.

The number of colors defined in the CLRCNTR color spectrum is always one greater than the specified number of contour levels. The number of colors that are actually available depends on the graphics hardware device that is used to display the plot. A color is assigned to a contour region based on the level of the contour line that generates that region. The increment in contour level that is used to assign the proper color to a contour region is calculated from the following equation:

$$\text{Increment} = (\text{max level} - \text{min level}) / (\text{no. of levels} - 1) \quad (2)$$

Because colors are assigned to contour regions and not to contour levels, all regions associated with the highest contour level are assigned the last color of the color spectrum. (All regions

associated with the lowest contour level could have been assigned the first color of the color spectrum just as easily.) Assigning the colors using this technique results in color two being assigned to the contour regions generated from contour level one, color three being assigned to the contour regions generated from contour level two, ..., and color $n + 1$ being assigned to the contour regions generated from contour level n . The entire plotting domain is displayed first, and it is assigned a color that is associated with regions that are generated from contour levels that are less than the lowest contour level that is either specified or found, depending on which contour level specification option is selected. The relationship between contour levels, contour regions, and assigned colors is as follows:

	Contour Level 1	2	3...	n-1	n		
Low End of Color Spectrum	Contour Regions from Levels < 1	Contour Regions from Level 1	Contour Regions from Level 2	...	Contour Regions from Level n-1	Contour Regions from Level n	High End of Color Spectrum
	Color 1	2	3	...	n	n+1	

Another way of interpreting this relationship is that contour regions that are generated from a specific contour level are always defined to be on the side of the associated contour line that is in the positive gradient direction of the function that is being plotted (i.e., moving toward the low end of the color spectrum is associated with a negative gradient of the function, and moving toward the high end of the color spectrum is associated with a positive gradient of the function). The method that is used to generate contour regions from contour lines, except for those regions that are generated from contour lines that close back on themselves, inherently assures that these regions are assigned a color that is consistent with the relationship between contour levels, contour regions, and assignment of colors. For regions that are generated from contour lines that close back on themselves, the proper color is assigned by using the following procedure:

The derivative of the function that is being plotted is computed along a unit normal vector assumed to point in the outward direction (i.e. away from the center of the contour region in question) at a random location on the associated closed contour line. If the area of the region, computed as described earlier, is greater than zero, then the assumed direction of the unit normal vector is correct. If the area of the region is less than zero, then the direction of the unit normal vector is toward the center of the contour region in question. The direction of this derivative characterizes the behavior of the function in the neighborhood of the closed contour line, and the proper color is assigned to the associated region.

3.0 PROGRAM APPLICATIONS

CLRCNTR has been interfaced with several CFD codes at the AEDC, and three applications are presented. All CFD computations were performed on the AEDC CRAY® X-MP/12 computer.

3.1 HYPERSONIC VISCOUS SHOCK-LAYER FLOW OVER A HEMISPHERE

A hypersonic viscous shock-layer, perfect-gas computation was performed over a hemisphere immersed in a Mach 22 free stream using the CVEQ (Ref. 11) code. The wall enthalpy to free-stream total enthalpy ratio was 0.13, and the free-stream static temperature was 390°R. The free-stream Reynolds number, based on nose radius, was 870,000. CVEQ is a computer code capable of solving the viscous shock-layer equations for the laminar flow of a perfect gas or air in thermodynamic equilibrium over a hemisphere in a supersonic or hypersonic free stream.

3.2 SUPERSONIC VISCOUS FLOW OVER A BLUNT FIN PROTRUDING FROM A FLAT PLATE

The three-dimensional, time-dependent, Navier-Stokes code, BLUNTFIN (Ref. 12), was used to compute the flow field over a blunt fin protruding from a flat plate immersed in a Mach 2.95 free stream. The configuration is identical to the configuration used by Hung and Buning (Ref. 8). The free-stream Reynolds number, based on fin width, was 271,000, and the free-stream static temperature was 195°R. An adiabatic wall condition was invoked during the computation. BLUNTFIN, a time-dependent, finite-volume computer code written in generalized body-fitted coordinates, is capable of predicting the viscous, compressible flow over a 3-D arbitrary geometry.

3.3 HYPERSONIC VISCOUS GAS JET NOSETIP FLOW FIELD

The flow field resulting from a sonic nose jet issuing counter to a Mach 15.8 free stream was computed using the gas jet nosetip (GJNT) code of Fox (Ref. 13). The nose jet was at 1-deg angle-of-attack relative to the free-stream velocity. The free-stream unit Reynolds number was 106,000,000 per foot, and the free-stream static temperature was 520°R. An adiabatic wall condition was invoked during the computation, and the gas jet total pressure divided by the total pressure downstream of a normal shock at a free-stream Mach number of 15.8 was 1.15. GJNT is a computer code capable of solving the three-dimensional, time-dependent, thin-layer Navier-Stokes equations for the laminar or turbulent flow field resulting from a

sonic nose jet issuing counter to a supersonic or hypersonic free stream. The code uses shock fitting to determine the location of the bow shock and dynamically adjusts the outer edge of the computational domain to coincide with the bow shock.

4.0 DISCUSSION OF RESULTS

DISSPLA (Ref. 14) plotting software was used in the CLRCNTR computer program, making the routine virtually hardware-device independent. All plots were generated on the Tektronix® 4115B color graphics workstation; display time was approximately 4 min per plot. Contour level option "1" was used, and thirteen contour levels were specified for all applications. Execution time for CLRCNTR was less than 60 sec on the CRAY X-MP/12 computer.

Contour plots of normalized static pressure, static temperature, stream function, local Mach number, total velocity, and total pressure are presented in Fig. 1 for the hypersonic viscous shock-layer flow over a hemisphere. Starting from the lower left corner of the plot and moving in a counter-clockwise direction, the four plotting domain boundaries are (1) the hemisphere axis-of-symmetry at the stagnation point, (2) the surface of the hemisphere, (3) the outflow plane at the shoulder of the hemisphere, and (4) the bow shock. The expansion of the flow around the hemisphere is easily perceived by observing, for example, the static pressure and static temperature plots. The interface lines between the different colors in the stream function plot represent the stream lines of the flow, and the difference in magnitude between two adjacent interface lines (i.e. stream lines) is a measure of the mass rate of flow between these two lines. The approximate location of the sonic line can be determined from the local Mach number plot. The stagnation region is visible in the total velocity plot, and the total pressure plot reveals a decreasing shock strength from the hemisphere axis-of-symmetry to the outflow plane.

The results of the blunt-fin application are presented in Figs. 2 and 3. Contour plots of normalized static pressure, density, static temperature, and local Mach number on the fin plane-of-symmetry are shown in Fig. 2. Starting from the lower left corner of the plot and moving in a counter-clockwise direction, the four plotting domain boundaries are (1) the surface of the flat plate, (2) the leading edge of the fin, (3) the outer edge of the computational domain, and (4) the inflow plane. The same parameters are plotted on the surface of the flat plate and are shown in Fig. 3. Starting from the lower left corner of this plot and moving in a counter-clockwise direction, the four plotting domain boundaries are (1) the fin plane-of-symmetry, (2) the surface of the blunt fin, (3) the outflow plane, and (4) the inflow plane. The important flow features to observe in the static pressure contour plot of Fig. 2 are the existence of a peak pressure on the fin leading edge, the appearance of an extreme low-pressure

region below this peak pressure, and an increase in the pressure toward the plate surface below this low-pressure region. Flow attributes related to these features are visible in the density, static temperature, and local Mach number contour plots on the fin plane-of-symmetry. In addition, embedded regions of lower static temperature and higher local Mach number appear, in their respective plots, upstream of the fin leading edge near the flat plate surface. Hung and Buning (Ref. 8) suggest that this behavior results from the presence of two embedded, reverse-flow, supersonic zones—one on the fin and another on the plate. They also suggest that the existence of these embedded regions is traced to a horseshoe vortex occurring in the flow field. The fin bow shock and its effect on the incoming flow are visible in the contour plots of Fig. 3. The bow shock causes the boundary layer on the flat plate to separate from the plate surface ahead of the fin, resulting in a separated flow region. This region consists of a lambda shock in the plane-of-symmetry and a horseshoe vortex near the plate surface. The lambda shock impinges on the fin bow shock and causes the increase in static pressure, density, and static temperature on the fin leading edge, observed in the symmetry plane contour plots of Fig. 2.

The results of the gas jet nosetip application are presented in Fig. 4. Starting from the lower right corner of the plot and moving in a clockwise direction, the four plotting domain boundaries are (1) the fitted bow shock; (2) the leeside outflow plane; (3) the leeside surface of the nosetip, the jet exit plane, and the windside surface of the nosetip; and (4) the windside outflow plane. The plotting domain is generated in the pitch plane-of-symmetry of the flow field. The free stream is compressed as it crosses the bow shock and perceives the nose jet as a protrusion. The nose jet first expands upstream from the exit plane and then is compressed until it stagnates against the incoming flow where it is turned downstream. The free stream, after being compressed subsonically by the bow shock, expands around the protrusion of the jet and accelerates down the body. A recirculating flow region is visible at the lip of the nosetip surface adjacent to the jet exit plane on both the windside and the leeside of the configuration. The flow attaches to the nosetip surface downstream of this region. The cooling effect of the gas jet is apparent from the normalized total enthalpy plot, where it is observed that the nosetip surface is sheathed by a relatively low-energy fluid layer.

5.0 CONCLUDING REMARKS

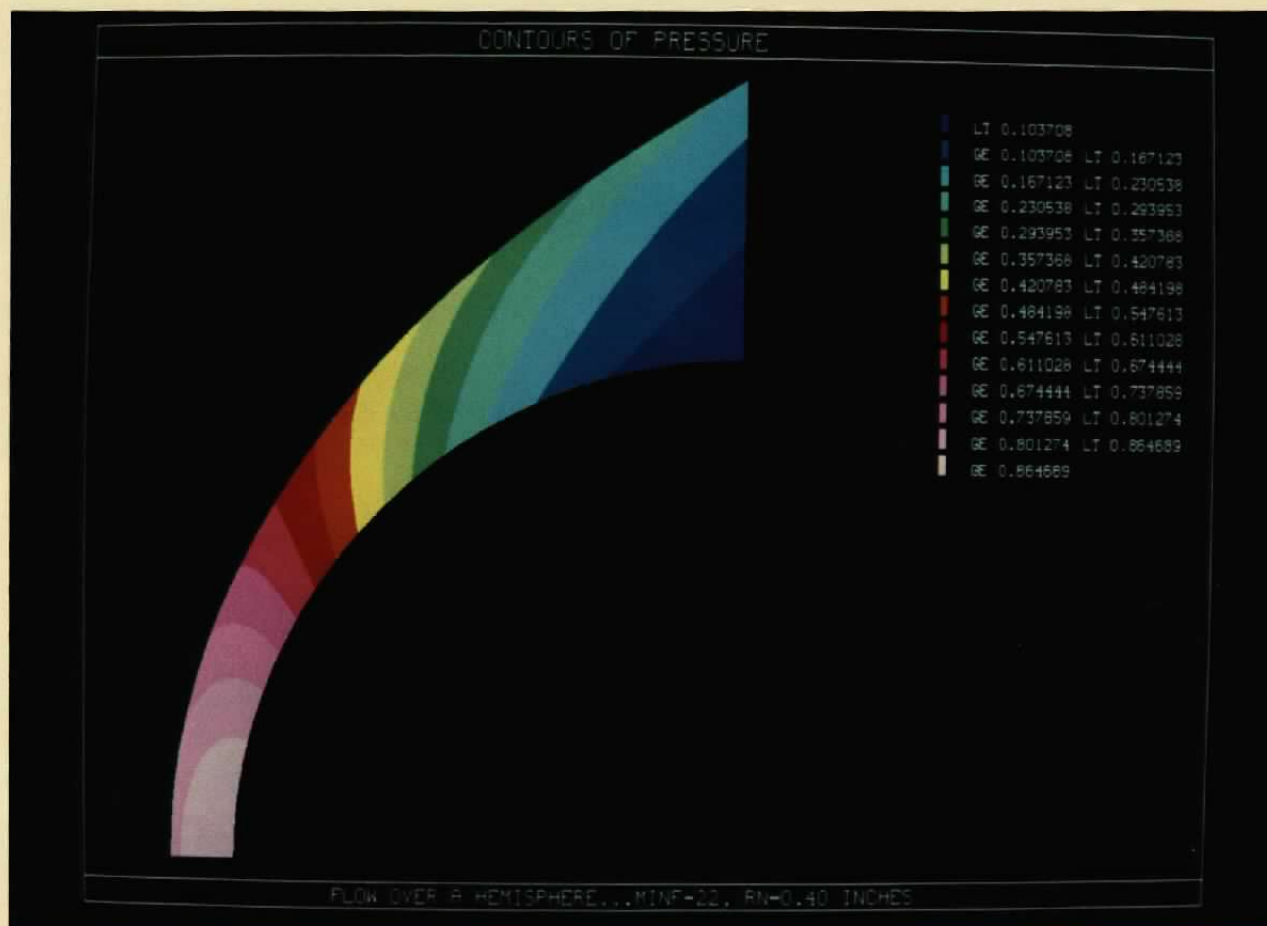
A computer program has been developed for displaying flow-field color contour plots generated from CFD solutions. The results from three different CFD codes have been presented to illustrate the capabilities and flexibility of the plotting routine. It is concluded that the program can adequately generate color contour plots of the flow field predicted by CFD codes and that these plots can be used effectively to interpret and evaluate the CFD results.

In addition, it is concluded that color helps to maintain the graphic clarity of the plot and facilitates the interpretation of the results by highlighting significant features of the flow.

REFERENCES

1. Ernst Mach Institut, Eckerstrasse 4, 78 Freiburg- im-Breisgau, Br., German Federal Republic.
2. Reynolds, O. "An Experimental Investigation of the Circumstances Which Determine Whether the Motion of Water Shall be Direct or Sinuous, and of the Law of Resistance in Parallel Channels." *Philosophical Transactions of the Royal Society of London*, 174, 1883, pp. 935-982, Scientific Papers 2, 51.
3. Prandtl, L. and Tietjens, O. "Hydro- und Aeromechanik." (Based on Prandtl's Lectures), Vols. I and II, Berlin 1929 and 1931, English translation by L. Rosenhead (Vol. I) and J. P. den Hartog (Vol. II), New York, 1934.
4. Wieselsberger, C. "Der Luftwiderstand von Kugeln." *Zeitschrift fur Metall Kunde*, Vol. 5, 1914, pp.140-144.
5. Van Dyke, M. *An Album of Fluid Motion*. The Parabolic Press, Stanford, California, 1982.
6. Deiwert, G. S. and Rothmund, H. "Three-Dimensional Flow Over a Conical Afterbody Containing a Centered Propulsive Jet: A Numerical Simulation." AIAA Paper No. 83-1709, Presented at the AIAA 16th Fluid and Plasmadynamics Conference, Danvers, Massachusetts, July 1983.
7. Chaussee, D. S., Rizk, Y. M., and Buning, P. G. "Viscous Computation of a Space Shuttle Flow Field." NASA TM 85977, June 1984.
8. Hung, C.-M. and Buning, P. G. "Simulation of Blunt-Fin Induced Shock Wave and Turbulent Boundary Layer Interaction." AIAA Paper No. 84-0457, Presented at the AIAA 22nd Aerospace Sciences Meeting, Reno, Nevada, January 1984.
9. Buning, P. G. and Steger, J. L. "Graphics and Flow Visualization in Computational Fluid Dynamics." AIAA Paper No. 85-1507, Presented at the AIAA 7th Computational Fluid Dynamics Conference, Cincinnati, Ohio, July 1985.

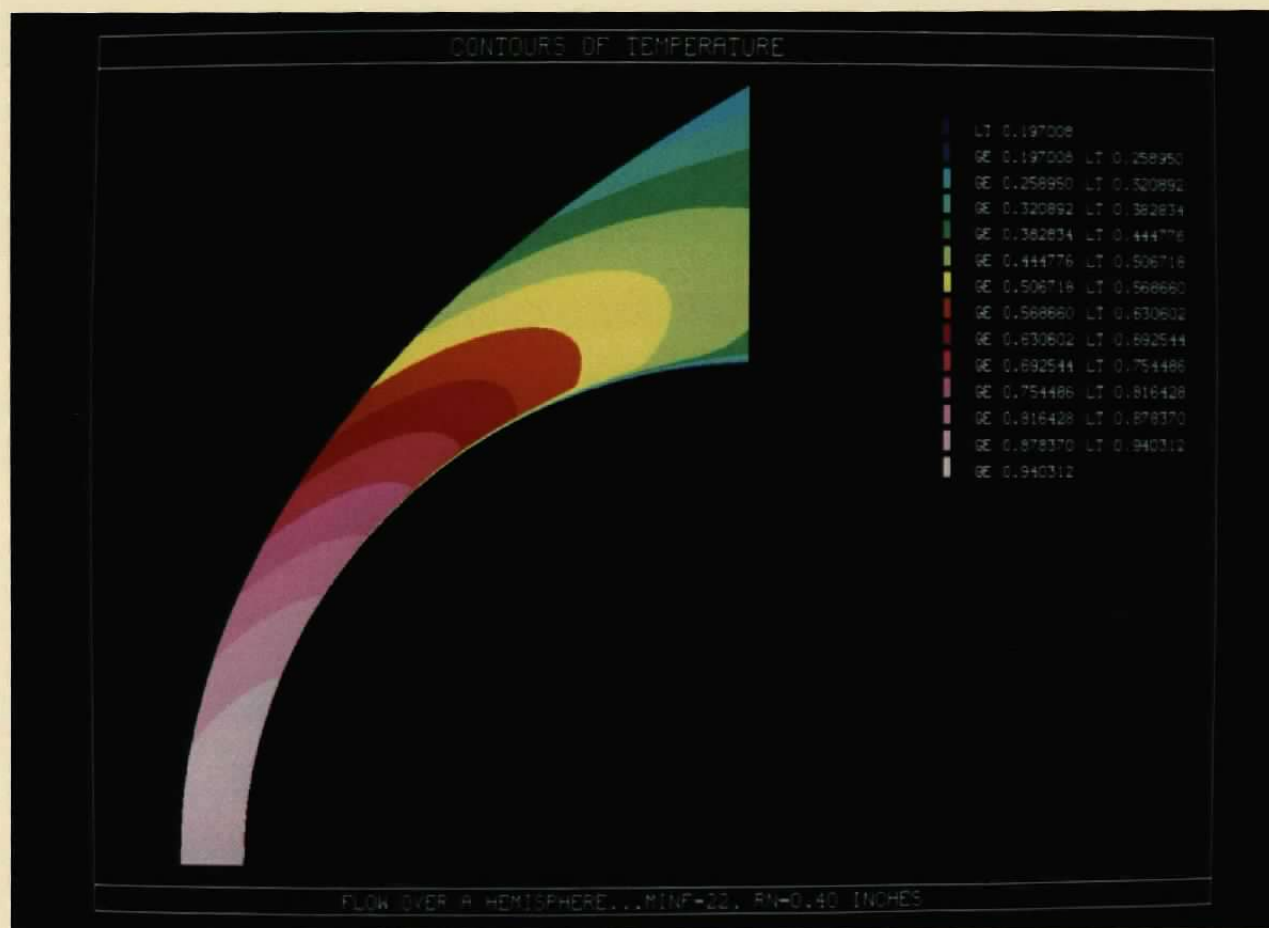
10. Hindman, R. G. "Modifications to MacCormack's 2-D Navier-Stokes Compression Ramp Code for Application to Flows with Axes of Symmetry and Wall Mass Transfer." AEDC-TR-80-24 (AD-A093742), January 1981.
11. Curtis, J. T. "Hemisphere Viscous Shock Layer Code for Equilibrium Air." AEDC-TR-82-22 (AD-B080027), January 1984.
12. Hung, C.-M. and Kordulla, W. "A Time-Split Finite-Volume Algorithm for Three-Dimensional Flow-Field Simulation." AIAA Paper No. 83-1957, Presented at the AIAA 6th Computational Fluid Dynamics Conference, Danvers, Massachusetts, July 1983.
13. Fox, J. H. "Counterflow Sonic Nosejet into a Supersonic Stream." AIAA Paper No. 86-1808, Presented at the AIAA 4th Applied Aerodynamics Conference, San Diego, California, June 1986.
14. Display Integrated Software System and Plotting Language (DISSPLA), User's Manual Current with Version 9.0, Integrated Software Systems Corporation, San Diego, California, 1981.



A E D C
14296-86

AEDC-TR-86-40

a. Normalized static pressure
Figure 1. Hypersonic viscous shock-layer flow over a hemisphere.



A E D C
14298-86

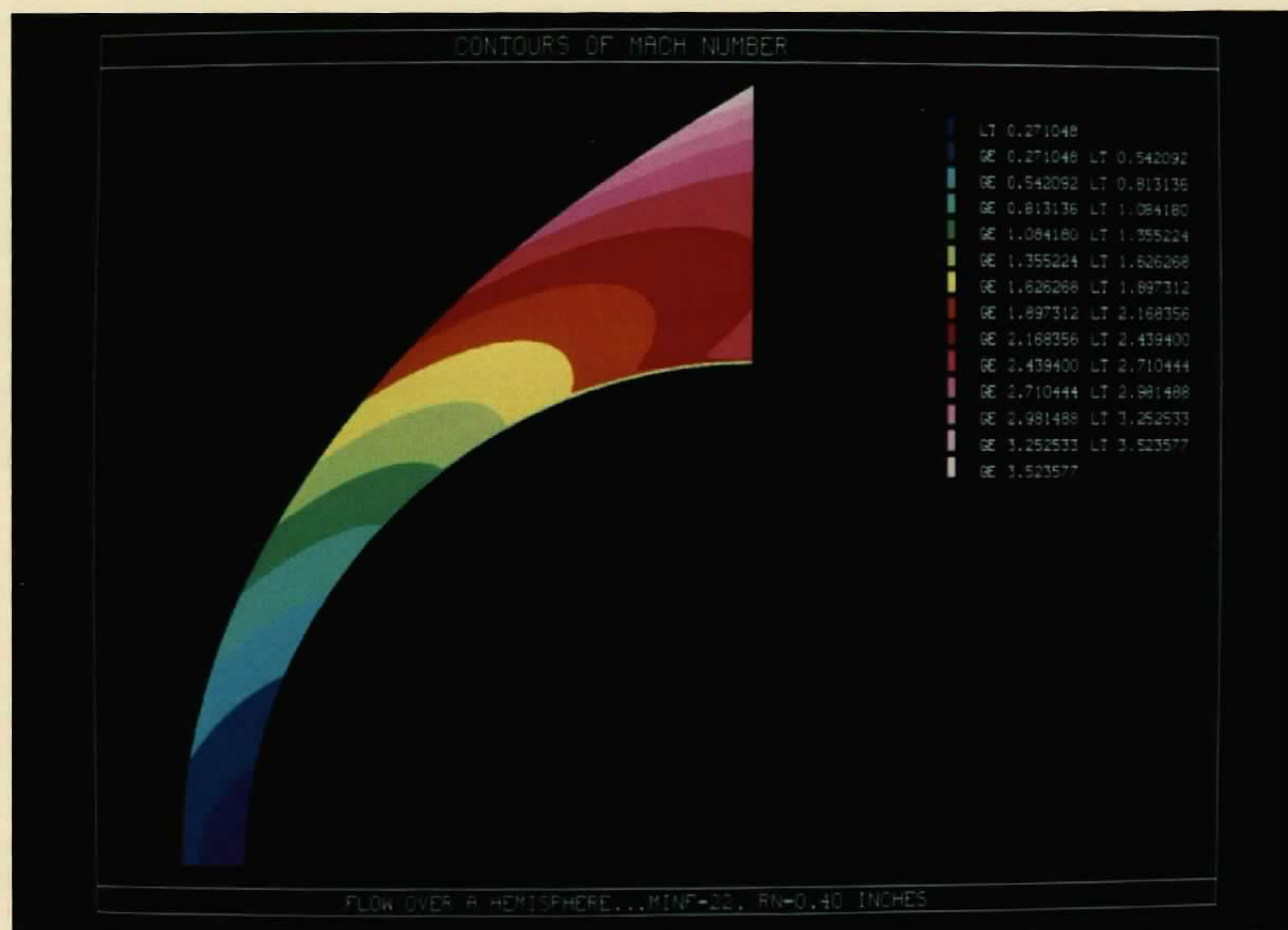
AEDC-TR-86-40

b. Normalized static temperature
Figure 1. Continued.



c. Normalized stream function
Figure 1. Continued.

A E D C
14299-86



A E D C
14300-86

AEDC-TR-86-40

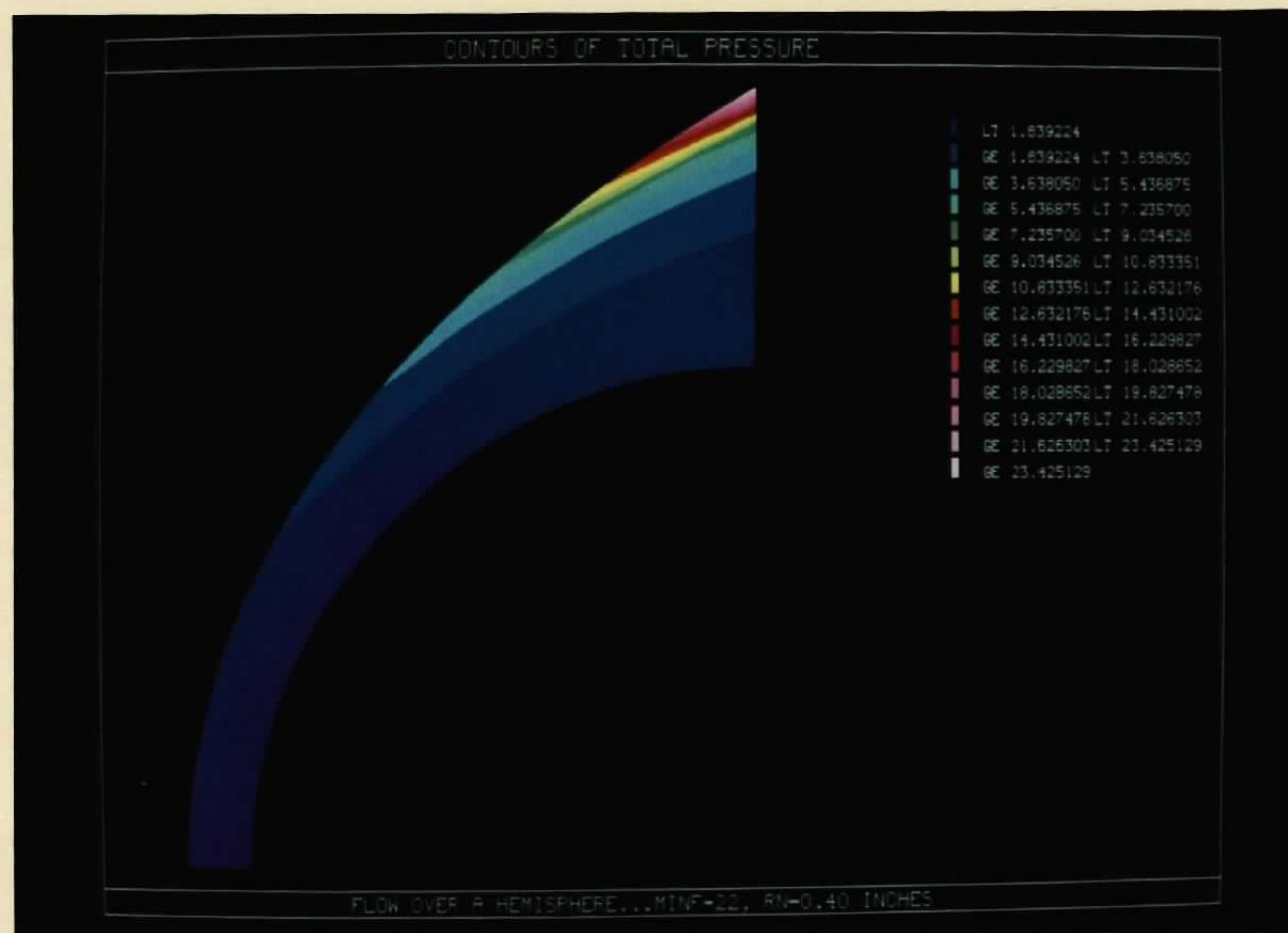
d. Local Mach number
Figure 1. Continued.



A E D C
14311-86

AEDC-TR-86-40

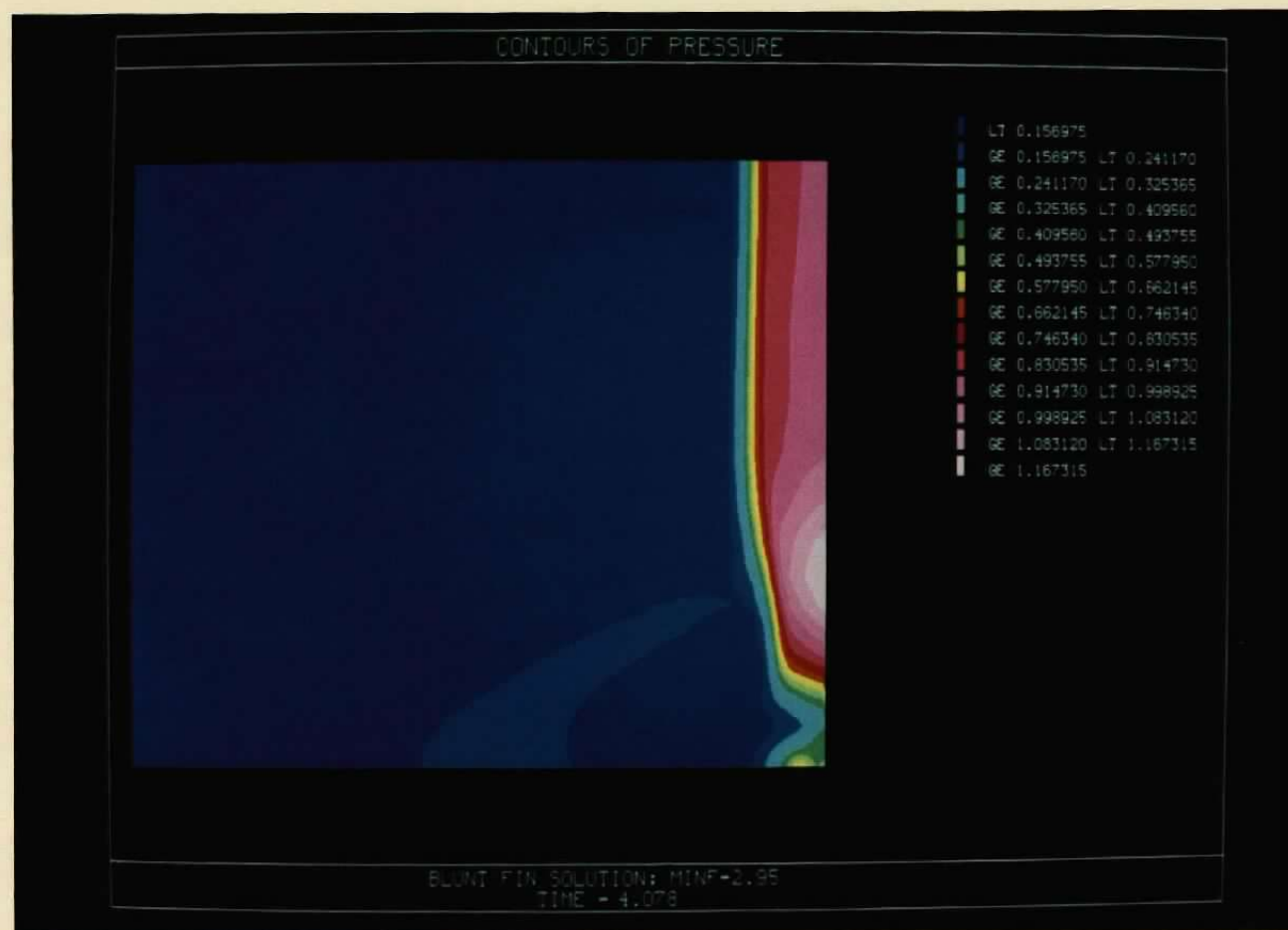
e. Normalized total velocity
Figure 1. Continued.



A E D C
14310-86

AE DC-TR-86-40

f. Normalized total pressure
Figure 1. Concluded.

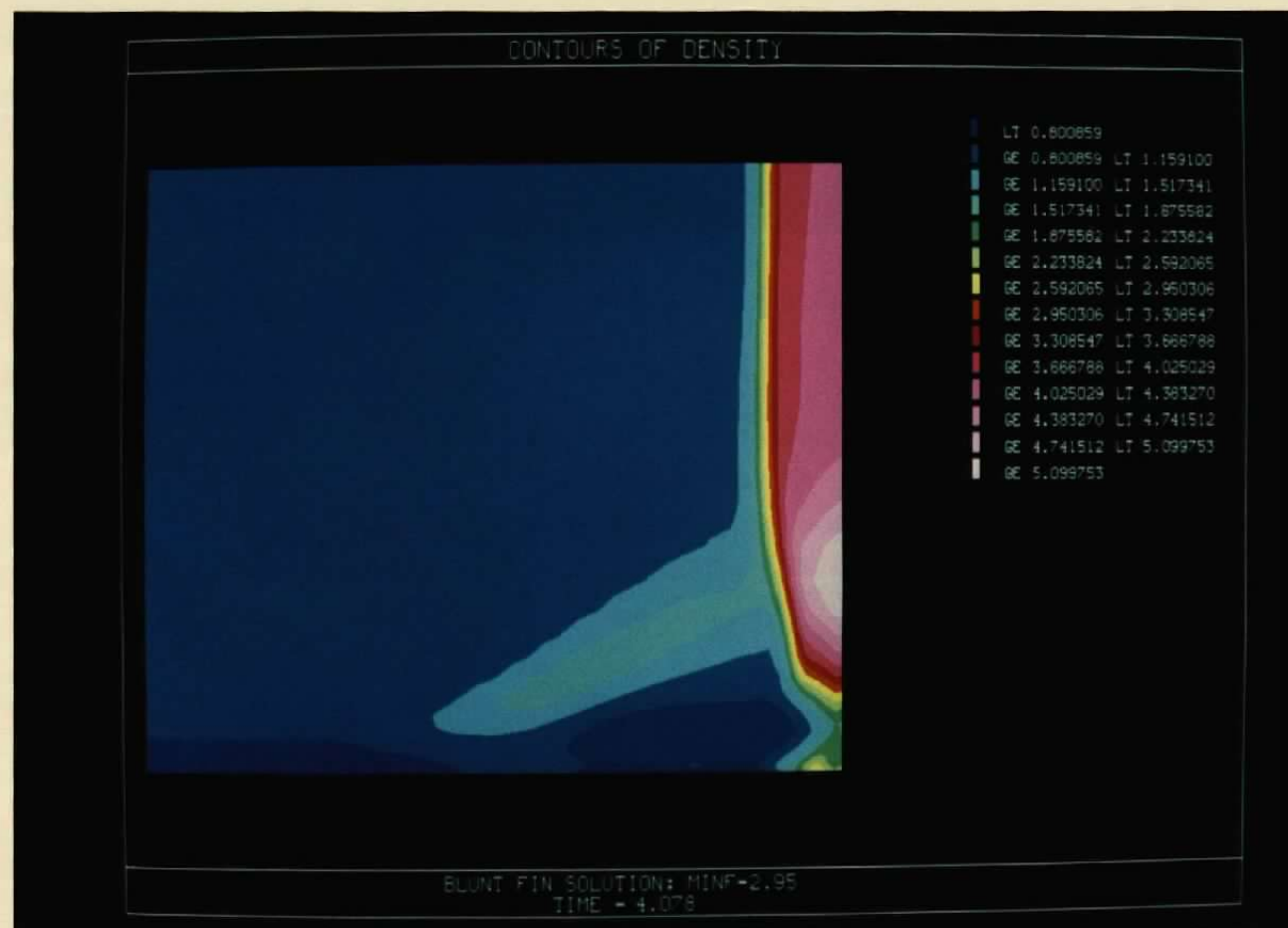


A E D C
14301-86

AEDC-TR-86-40

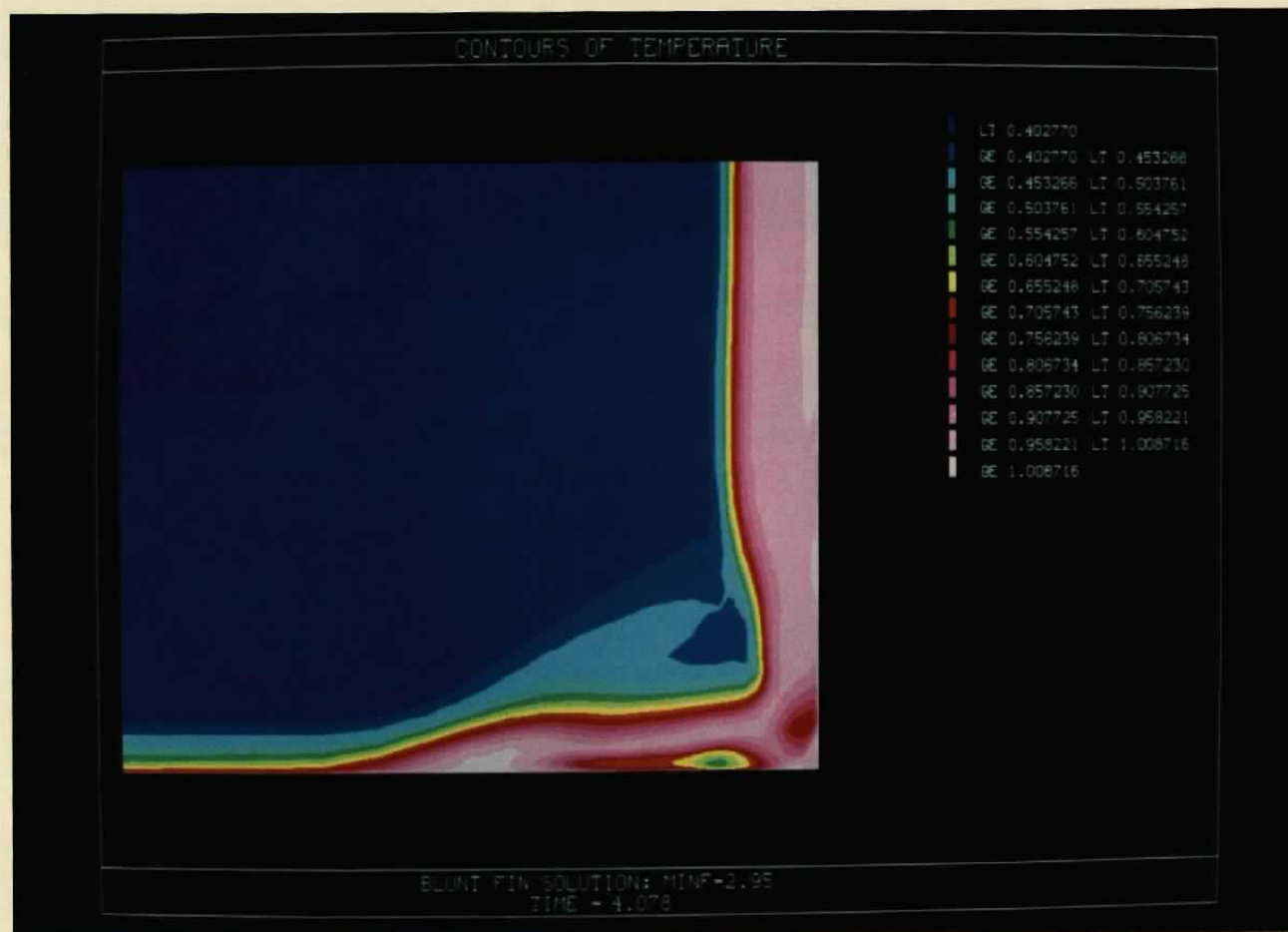
a. Normalized static pressure

Figure 2. Supersonic viscous flow over a blunt fin protruding from a flat plate (fin plane-of-symmetry).



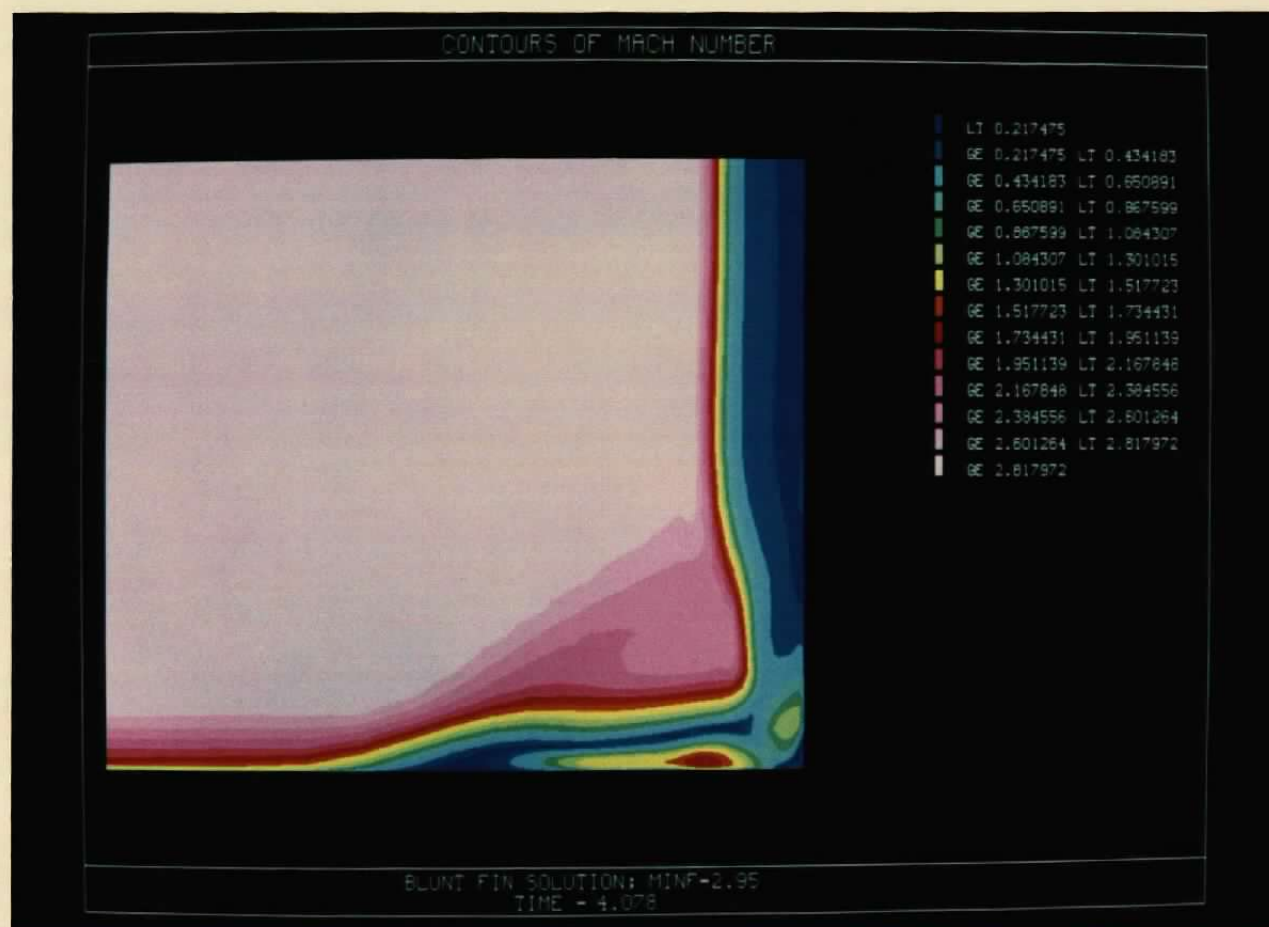
A E D C
14302-86

b. Normalized density
Figure 2. Continued.



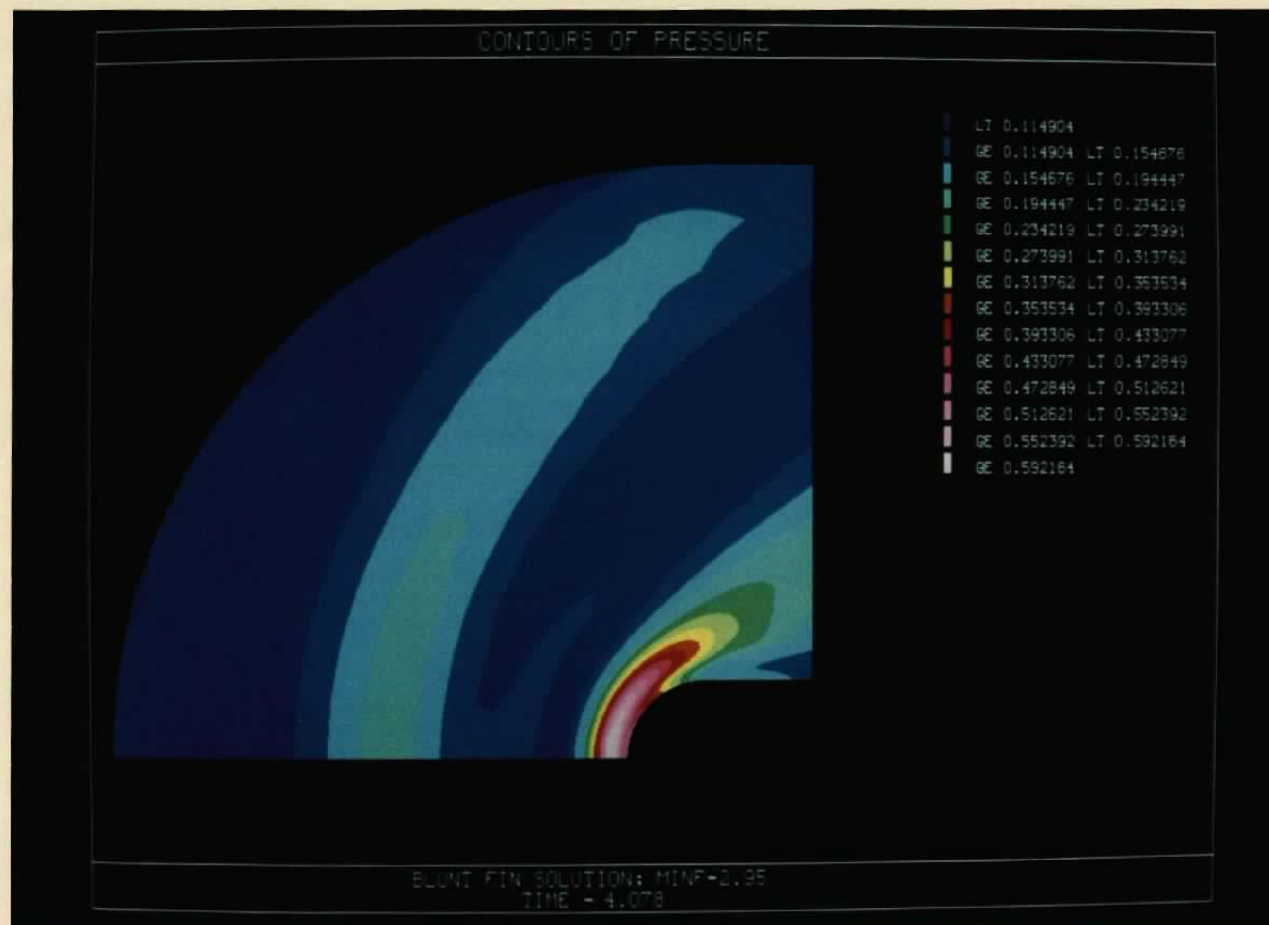
A E D C
14303-86

c. Normalized static temperature
Figure 2. Continued.



d. Local Mach number
Figure 2. Concluded.

A E D C
14304-86

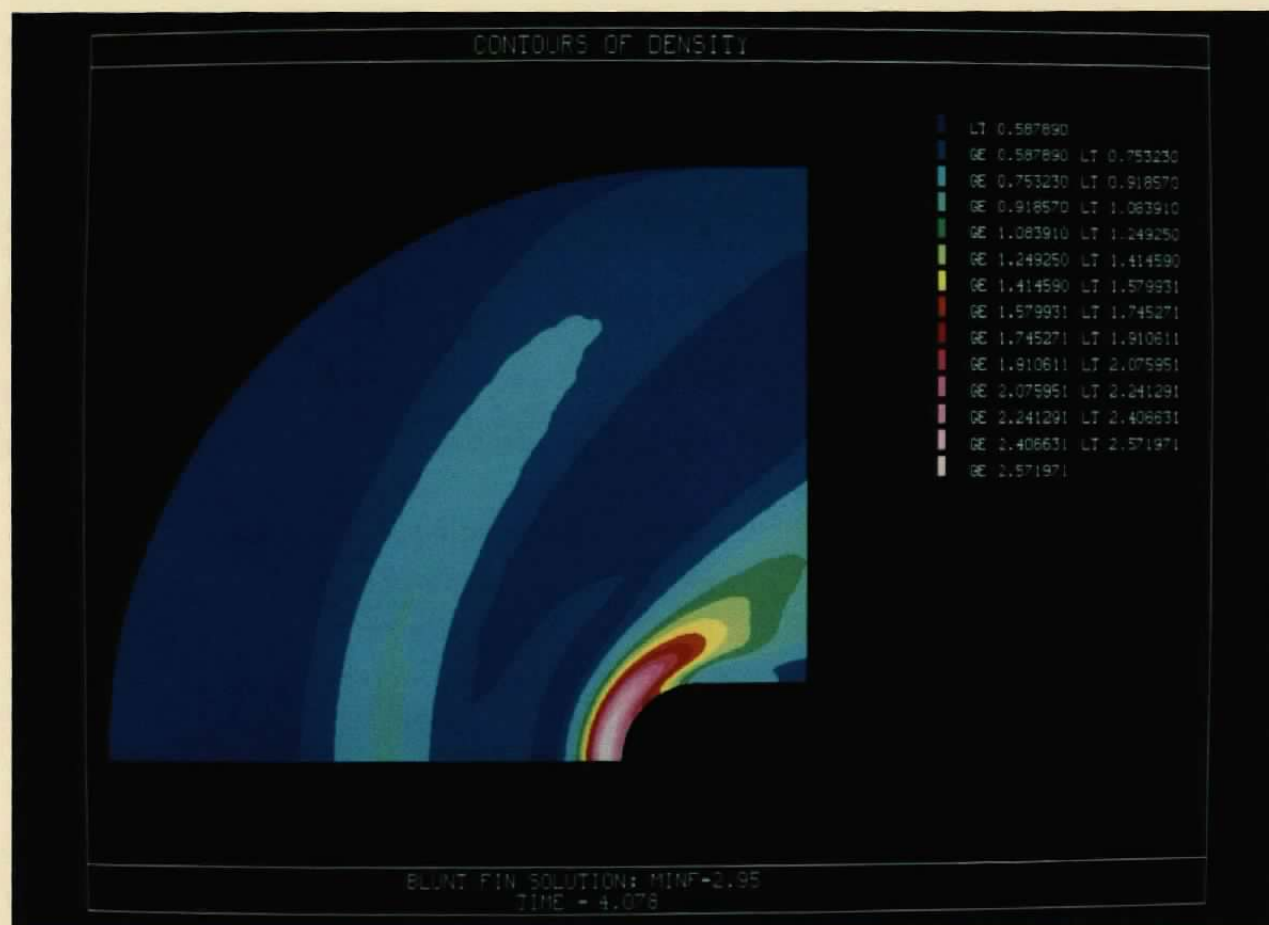


A E D C
14305-86

AEDC-TR-86-40

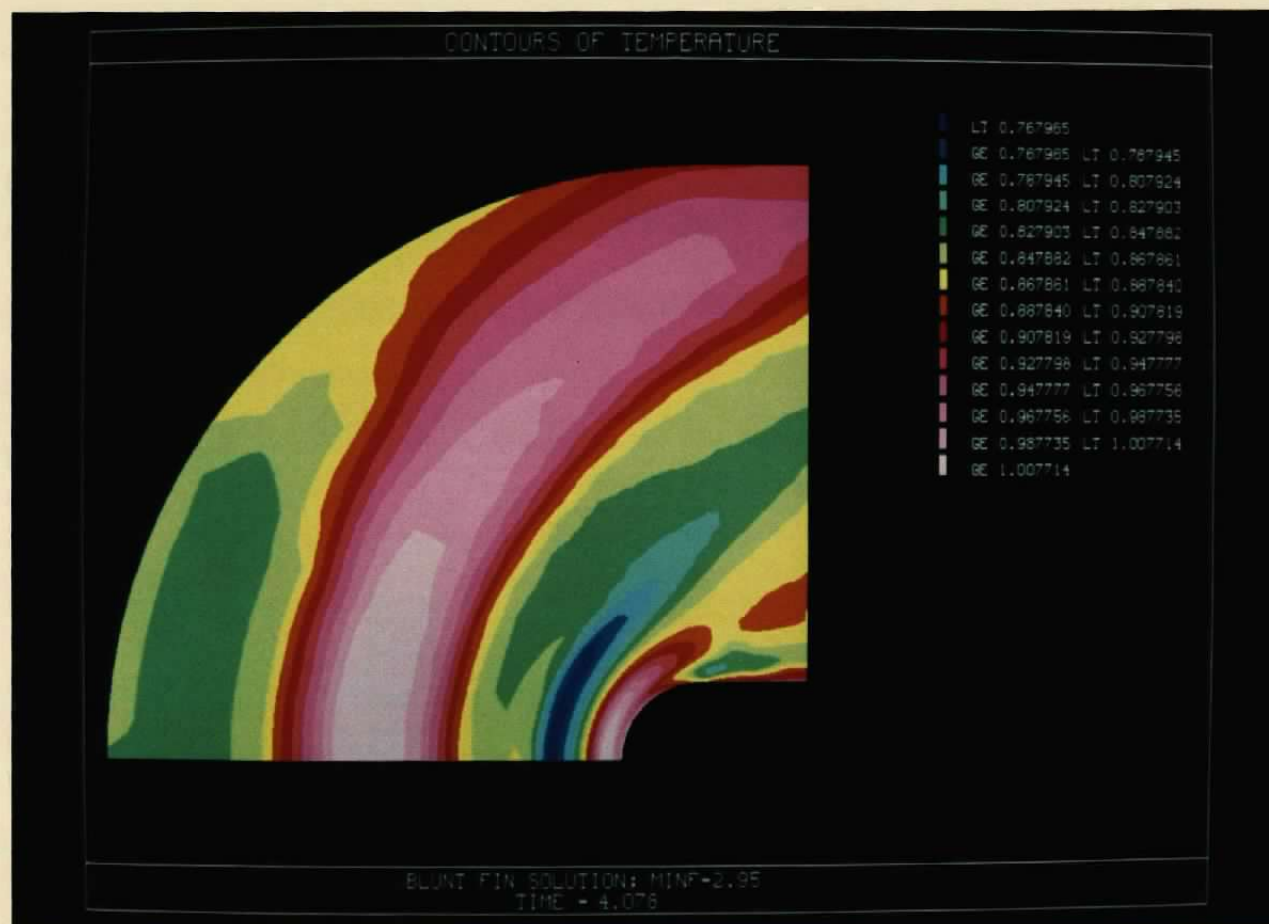
a. Normalized static pressure

Figure 3. Supersonic viscous flow over a blunt fin protruding from a flat plate (plate surface).



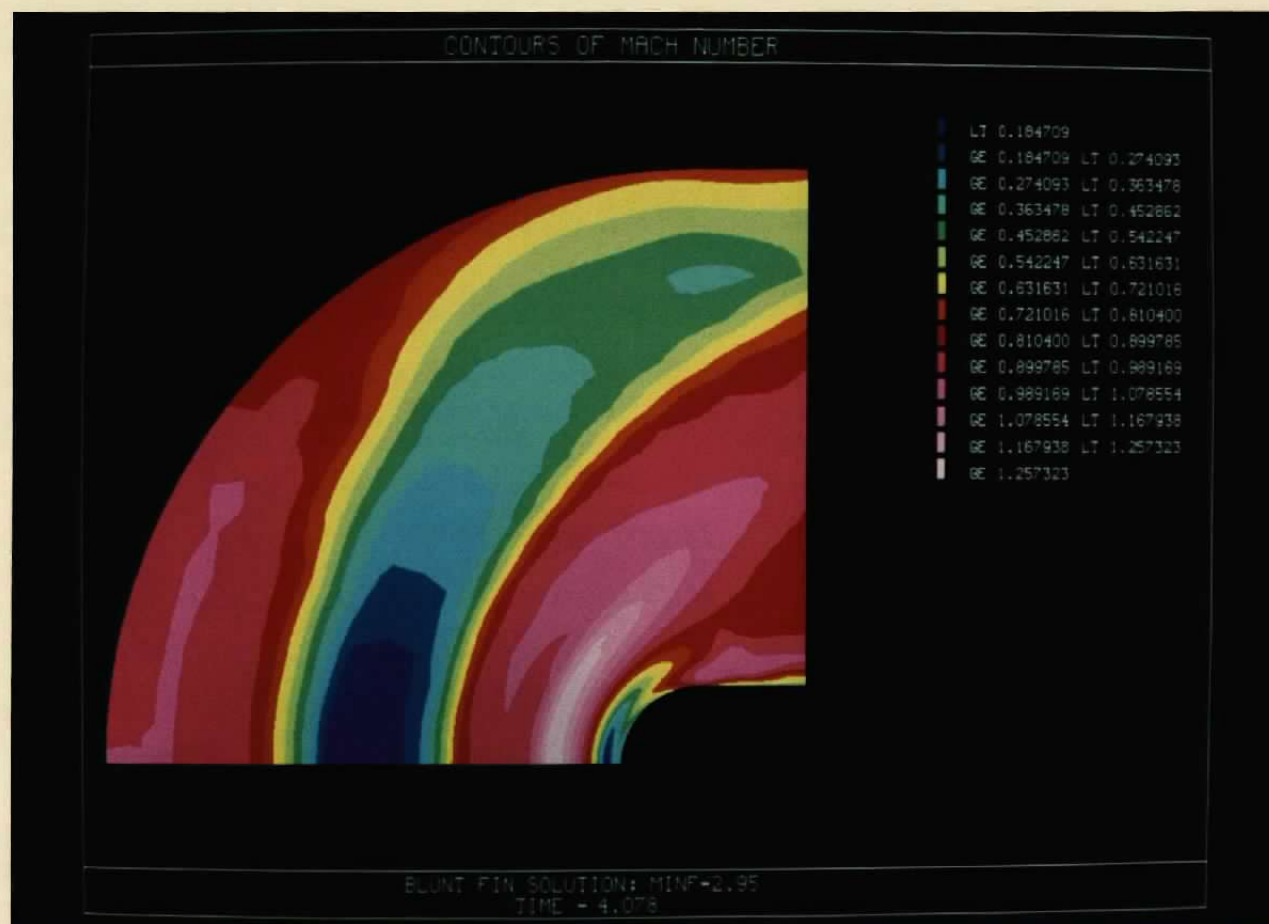
b. Normalized density
Figure 3. Continued.

A E D C
14307-86



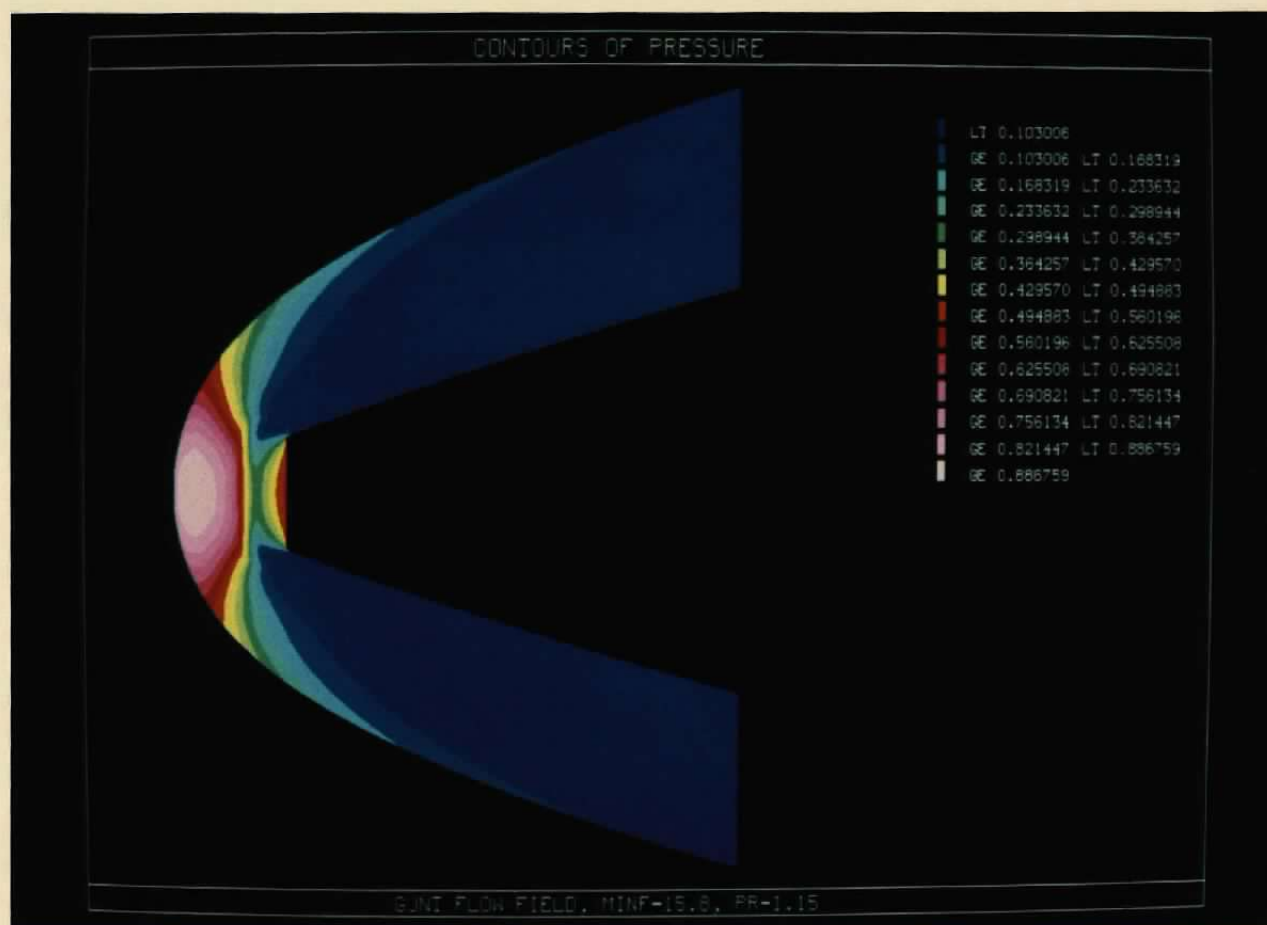
c. Normalized static temperature
Figure 3. Continued.

A E D C
14308-86



d. Local Mach number
 Figure 3. Concluded.

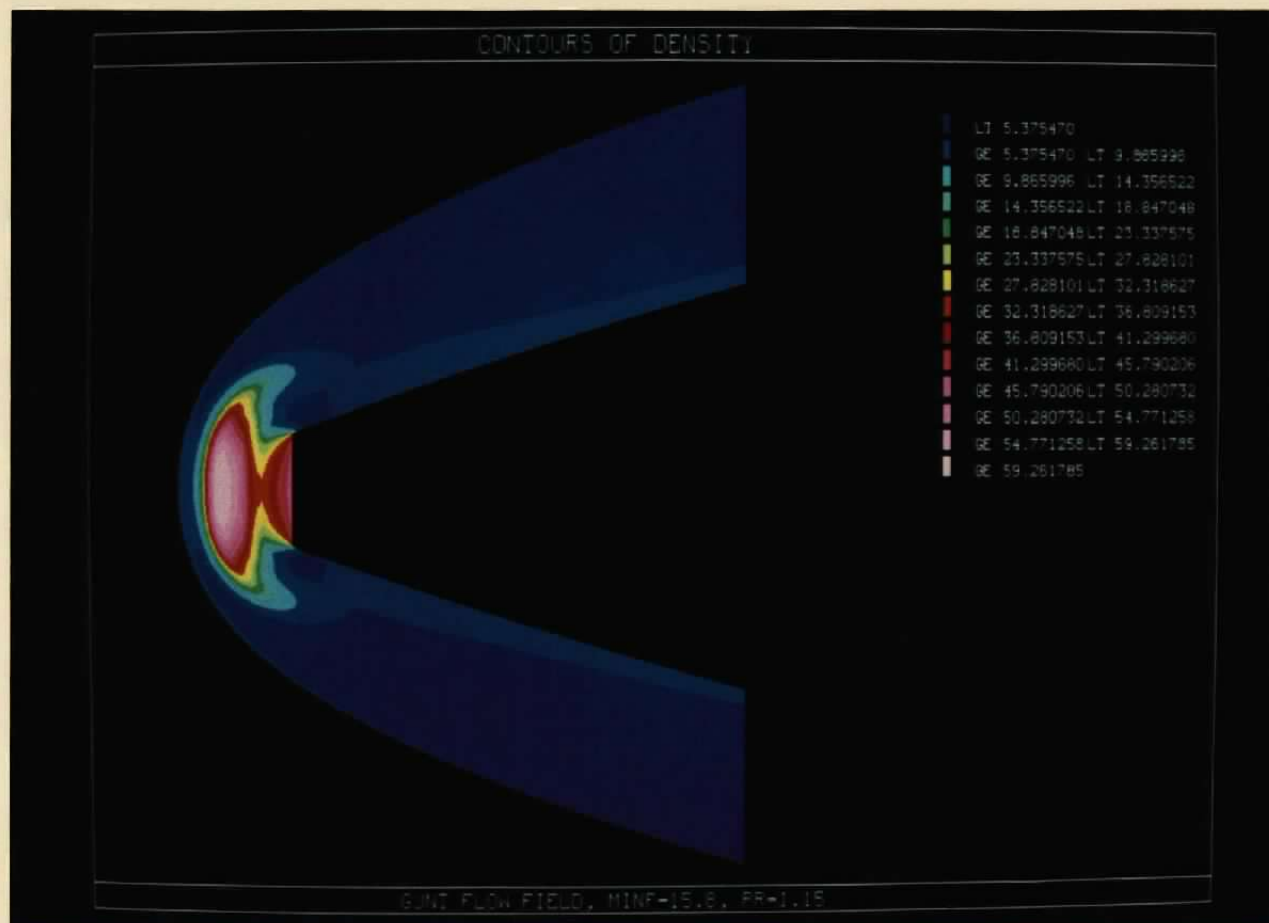
A E D C
 14309-86



A E D C
 7847-86

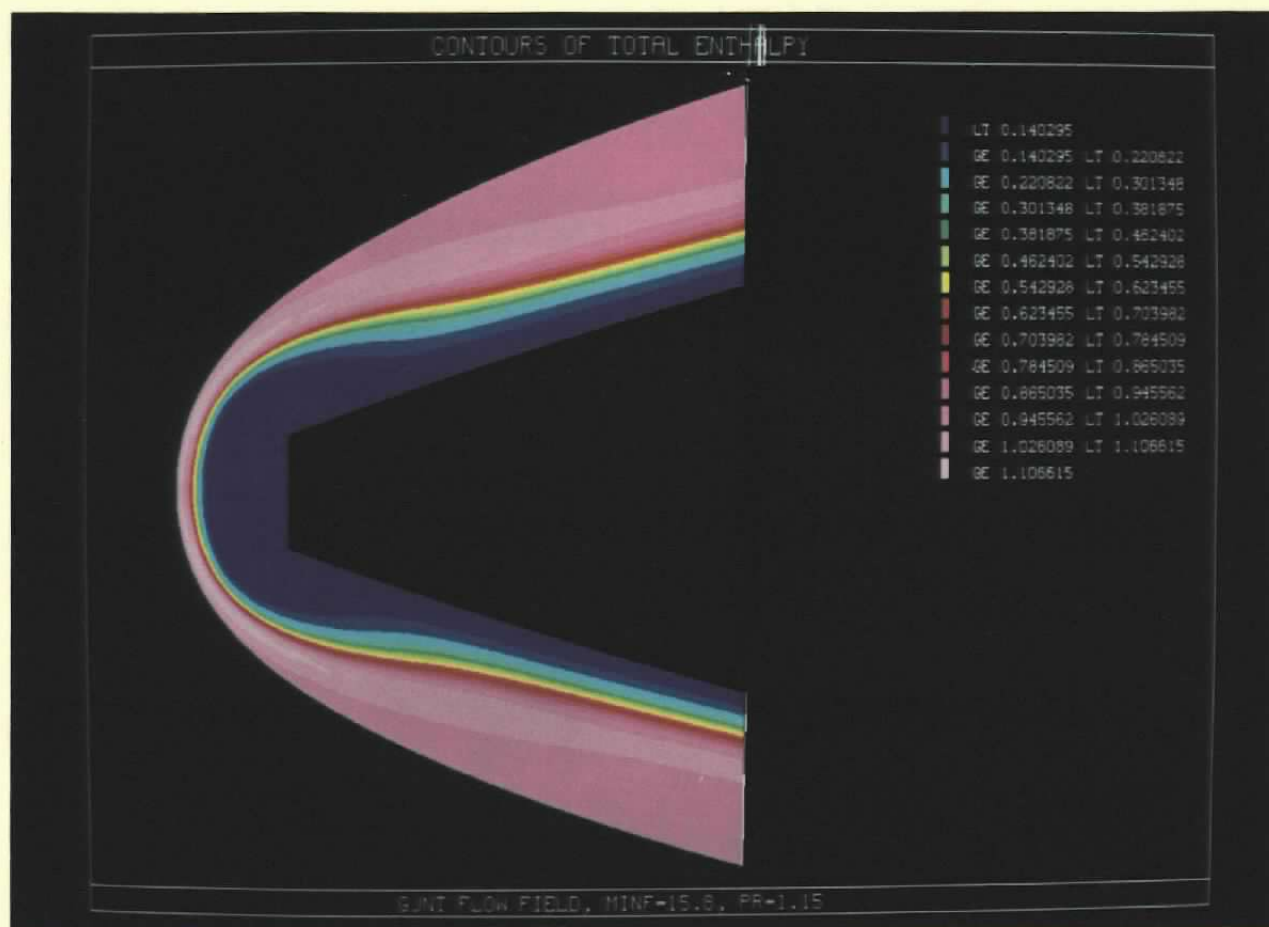
AEDC-TR-86-40

a. Normalized static pressure
 Figure 4. Hypersonic viscous gas jet nosetip flow.



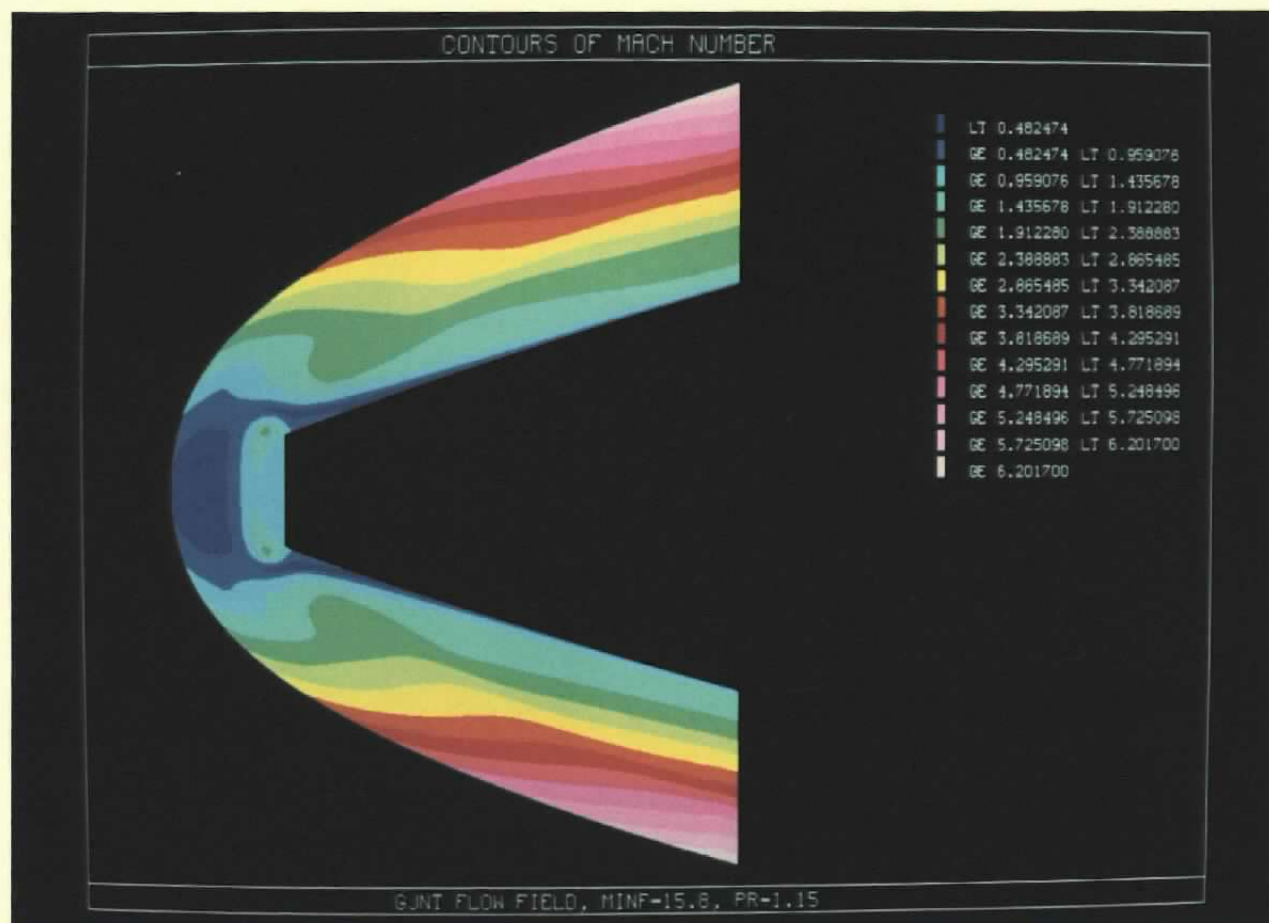
b. Normalized density
Figure 4. Continued.

AEDC
 7848-86



c. Normalized total enthalpy
Figure 4. Continued.

AEDC
7849-86



d. Local Mach number
Figure 4. Concluded.

A E D C
7850-86

NOMENCLATURE

delta	Increment of contour level
e	Energy per unit volume, normalized by $q_{\infty} U_{\infty}^2$
GE	Greater than or equal to
H	Enthalpy, normalized by $H_{o\infty}$
I	Index used in Eq. (1)
J	Grid point index in the longitudinal direction of the general plotting domain
JMAX	Total number of grid points in the longitudinal direction of the general plotting domain
K	Grid point index in the normal direction of the general plotting domain
KMAX	Total number of grid points in the normal direction of the general plotting domain
LT	Less than
M	Mach number
max	Maximum contour level
min	Minimum contour level
MINF	Free-stream Mach number
N	Upper index used in Eq. (1)
n	Number of contour levels or color number
PR	Jet pressure ratio
Re	Reynolds number

Rn	Nose radius, inches
s	Entropy, normalized by $s_{\infty} \gamma M_{\infty}^2$
T	Static temperature, normalized by $T_{o\infty}$
TIME	Elapsed integration time in BLUNTFIN code, normalized by the number of characteristic lengths traveled with the free-stream velocity
U	Total velocity, normalized by U_{∞}
u, v, w	Cartesian velocity components, normalized by U_{∞}
x, y, z	Cartesian coordinates of grid points, user-defined dimensions
γ	Ratio of specific heats
ρ	Density, normalized by ρ_{∞}

SUBSCRIPTS

cr	Critical value
o, t	Total quantities
∞	Free-stream quantities